DALTON
FULL PAPER

Synthesis and co-ordination chemistry of the compartmental tetradentate ligand bis[3-(2-pyridyl)pyrazol-1-yl]methane

Karen L. V. Mann,[a] John C. Jeffery,[a] Jon A. McCleverty,*[,a] Peter Thornton[b] and Michael D. Ward*[,a]

[a] *School of Chemistry, University of Bristol, Cantock's Close, Bristol, UK BS8 1TS*
[b] *Department of Chemistry, Queen Mary and Westfield College, Mile End Road, London, UK E1 4NS*

Reaction of 3-(2-pyridyl)pyrazole with CH_2Br_2 and NaOH under phase-transfer conditions afforded the new ligand bis[3-(2-pyridyl)pyrazol-1-yl]methane (L), containing two bidentate pyrazolyl-pyridine arms linked to a methylene spacer. The crystal structure of $L\cdot 4H_2O$ revealed a complicated network of hydrogen bonding between stacks of ligands and interspersed chains of water molecules. Reaction of L with Co^{II}, Ni^{II}, Cu^{II} and Zn^{II} gave in every case a centrosymmetric dinuclear complex of the type $[M_2L_2(\mu\text{-}X)_2]^{2+}$ (X = hydroxide or monodentate acetate). Three of the four complexes were crystallographically characterised and have the same basic core structure. The $M_2(\mu\text{-}X)_2$ core is spanned by two bridging ligands L, each of which co-ordinates one bidentate arm to each metal. The two ligands are co-ordinated in an achiral 'face-to-face' mode rather than the alternative helical mode; this leaves space between the two metal ions for the monodentate ligands X, which would not be possible with a helical arrangement of ligands. The electronic spectral properties of the Co^{II}, Ni^{II} and Cu^{II} complexes are consistent with the pseudo-octahedral N_4O_2 co-ordination geometries seen in the crystal structures. Magnetic susceptibility studies on $[Cu_2L_2(\mu\text{-}OH)_2][PF_6]_2$ show an antiferromagnetic interaction with a singlet–triplet splitting $2J$ of $-110\ cm^{-1}$, very different from that expected on the basis of the structural parameters of the $Cu_2(\mu\text{-}OH)_2$ core due to the additional pathway for magnetic exchange provided by the bridging ligands L. In contrast, in the mononuclear complex $[PbL_2][ClO_4]_2$ the ligands L are tetradentate chelates, giving the metal centre an eight-co-ordinate geometry which is very irregular due to the additional presence of a stereochemically active lone pair. In $[In_2LCl_4(\mu\text{-}OH)_2]$, L reverts to its more usual bridging mode. This complex contains two pseudo-octahedral In^{III} centres with *cis*,*cis*,*cis*-$N_2O_2Cl_2$ co-ordination environments, and is a rare example of hydroxide ligands bridging two In^{III} centres.

We describe in this paper the preparation of the new ligand bis[3-(2-pyridyl)pyrazol-1-yl]methane (L, Scheme 1) and its co-ordination chemistry with the first-row transition-metal dications Co^{II}, Ni^{II}, Cu^{II} and Zn^{II}, as well as the two p-block metal ions In^{III} and Pb^{II}. Ligand L is typical of a class of ligand in which two multidentate chelating 'arms' are linked by a central bridge, in this case a CH_2 spacer. Such ligands have the ability to co-ordinate all of their donor atoms to a single metal ion if it is sufficiently large,[1] or to act as a bridge between different metal ions to give polynuclear complexes, which are often found to have helical topologies.[1–3] 'Face-to-face' (achiral) arrangements of bridging ligands in complexes of such ligands are also known, and the factors which influence formation of helical or face-to-face complexes have been investigated.[4]

There are two principal reasons for this work. Firstly, we[5] and others[6] have observed that with simple potentially bridging ligands of this type, structurally highly sophisticated compounds can form whose architectural complexity may be out of all proportion to the simplicity of the component parts. The subtle interactions that control the assembly of such complexes may be rationalised after the event but can rarely be predicted in advance.[7] For this reason the preparation and structural characterisation of metal complexes of these bridging ligands will help our eventual understanding of the factors which control their sometimes unusual structures. Secondly, polynuclear complexes in general are of wide interest because of the unusual fascinating electronic[8] and magnetic[9] properties known to be associated with polynuclear (as opposed to mononuclear) complexes, as well as their occurrence in metalloprotein active sites where the catalytic function depends on cooperation between two or more metal centres.[10]

Accordingly, we have recently prepared a series of related potentially bridging ligands and studied their co-ordination chemistry.[1,3,5] The general synthetic route to these is straightforward, involving initial preparation of a multidentate 'arm'

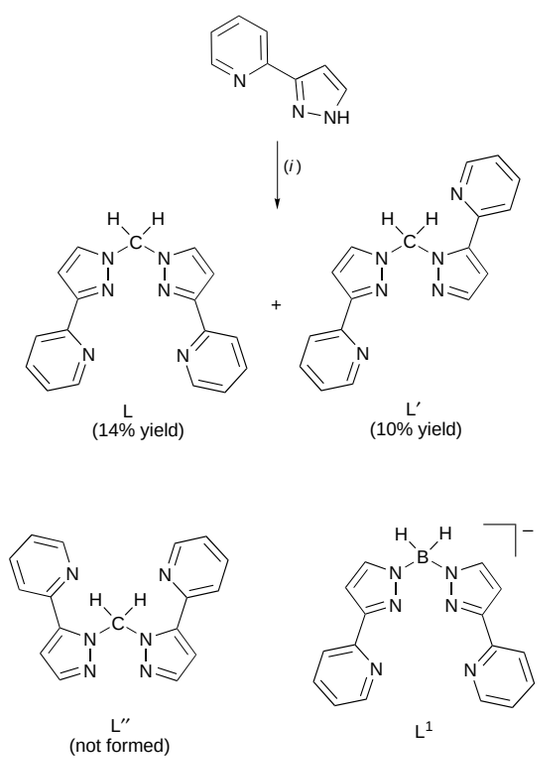

Scheme 1 (*i*) $0.5CH_2Br_2$, NaOH, NBu_4Br, H_2O, toluene

containing a terminal pyrazolyl ring; the pyrazolyl rings can then be attached to one of a variety of bridging groups such as tetrahydroborate, phosphinate, and (now) methylene. The parent bis(pyrazolyl)methane (bpm) was first prepared by Trofimenko,[11] and since its introduction, it and its simple alkyl-substituted derivatives have been used in both co-ordination and organometallic chemistry.[12] Derivatives of bpm have been prepared in which an additional donor group is attached to the methylene carbon atom, as in (2-thienyl)bis(pyrazolyl)-methane[13] and (2-hydroxyphenyl)bis(pyrazolyl)methane,[14] which are both potentially terdentate capping ligands with NNS and NNO donor sets respectively. However L is to our knowledge the first example of a bpm derivative in which additional co-ordinating groups (2-pyridyl substituents) have been attached to the pyrazolyl rings to afford a ligand with two chelating arms attached by a methylene spacer.

Experimental

General details

Instrumentation used for routine spectroscopic and electrochemical studies has been described previously.[15] 3-(2-Pyridyl)pyrazole was prepared by the published method.[16] Commercial reagents were used without further purification. Magnetic susceptibilities were measured over a range of temperatures down to 77 K using a Faraday balance calibrated with $HgCo(NCS)_4$ as described previously.[17]

Preparation of bis[3-(2-pyridyl)pyrazol-1-yl]methane L

This preparation is based on a recent synthesis of unsubstituted bis(pyrazolyl)methane.[18] 3-(2-Pyridyl)pyrazole (10.0 g, 6.9 mmol), CH_2Br_2 (6.61 g, 3.8 mmol), aqueous NaOH (4.50 g dissolved in 10 cm^3 water) and tetra-*n*-butylammonium bromide (0.10 g, 0.31 mmol) were added to toluene (80 cm^3) and the mixture was heated to reflux overnight under N_2 with vigorous stirring. After cooling, the mixture was filtered and placed in a separating funnel. The organic phase was collected, dried ($MgSO_4$) and evaporated to dryness *in vacuo*. The crude product was purified by chromatography on flash silica, using CH_2Cl_2 containing 1–2% MeOH (v/v) as the mobile phase. After a fast-running by-product which eluted first, two main products eluted close together. The first of these to elute was L′, the positional isomer of L in which one pyrazolyl group is attached to the methylene bridge *via* N^2 rather than N^1 (see Scheme 1), isolated in 10% yield. The second of the two main products was the desired product L, isolated in 14% yield.

Data for L. Electron impact (EI) mass spectrum: $m/z = 302$ (M^+). ^{1}H NMR [300 MHz, $(CD_3)_2CO$]: δ 8.56 (2 H, ddd, *J* 4.9, 1.8, 0.9, pyridyl H^6), 8.02 (4 H, m, pyridyl H^3 and pyrazolyl H^5), 7.80 (2 H, td, *J* 7.7, 1.8, pyridyl H^4), 7.27 (2 H, ddd, *J* 7.5, 4.9, 1.2, pyridyl H^5), 6.94 (2 H, d, *J* 2.6 Hz, pyrazolyl H^4), 6.57 (2 H, s; CH_2) (Found: C, 67.4; H, 4.5; N, 27.2. Calc. for $C_{17}H_{14}N_6$: C, 67.5; H, 4.7; N, 27.8%).

Data for L′. EI mass spectrum: $m/z = 302$ (M^+). ^{1}H NMR [300 MHz, $(CD_3)_2CO$]: δ 8.82 (1 H, ddd, *J* 4.9, 1.8, 0.9, pyridyl H^{6A}), 8.51 (1 H, ddd, *J* 4.9, 1.8, 1.0, pyridyl H^{6B}), 7.95 (1 H, td, *J* 7.7, 1.8, pyridyl H^{4A}), 7.83 (3 H, m, 2 × pyridyl H^3 and pyrazolyl H^{5B}), 7.72 (1 H, td, *J* 7.7, 1.9, pyridyl H^{4B}), 7.58 (1 H, d, *J* 1.8, pyrazolyl H^{5A}), 7.45 (1 H, ddd, *J* 7.5, 4.9, 1.2, pyridyl H^{5A}), 7.22 (1 H, ddd, *J* 7.4, 4.9, 1.3, pyridyl H^{5B}), 7.11 (2 H, s, CH_2), 6.83 (1 H, d, *J* 2.1, pyrazolyl H^4), 6.81 (1 H, d, *J* 2.4 Hz, pyrazolyl H^4). The labels A and B refer to the two inequivalent pyridyl/pyrazolyl arms; these were assigned by comparison with the spectrum of L, above in which both arms are of type B.

Preparations

Complexes with Co^{II}, Ni^{II}, Cu^{II} and Zn^{II}. All four complex preparations followed the same method. Equimolar amounts of L and the appropriate metal(II) acetate hydrate (typically 0.2 mmol of each) were dissolved in MeOH (10 cm^3) and the resultant solution stirred at room temperature for 1 h. Addition of an aqueous solution of KPF_6 (M = Ni, Cu or Zn) or $NaClO_4$ (M = Co) resulted in precipitation of the crude complexes which were filtered off, dried *in vacuo* and then recrystallised from MeCN–diethyl ether. The yields of recrystallised material were 30–50% but were not optimised.

$[PbL_2][ClO_4]_2$. A mixture of L (0.060 g, 0.20 mmol) and $Pb(NO_3)_2$ (0.066 g, 0.20 mmol) in MeOH (10 cm^3) was stirred to give a clear solution. Addition of aqueous $NaClO_4$ and overnight refrigeration resulted in precipitation of a white solid which was filtered off and dried (crude yield 50%). Recrystallisation from MeCN–diethyl ether afforded X-ray quality crystals.

$[In_2LCl_4(\mu\text{-}OH)_2]$. A mixture of L (0.050 g, 0.17 mmol) and $InCl_3{\cdot}4H_2O$ (0.016 g, 0.055 mmol) in MeOH (10 cm^3) was stirred to give a clear solution. After addition of water (10 cm^3) and further stirring for 1 h a white precipitate formed which was filtered off and dried to give the crude product in 70% yield. X-Ray quality crystals were grown by slow evaporation of a dimethylformamide (dmf) solution of the crude material.

Analytical and mass spectroscopic data for all of the complexes, and electronic spectral data for the transition-metal complexes, are collected in Table 1.

Crystallography

Suitable crystals were quickly transferred from the mother-liquor to a stream of cold N_2 at −100 °C on a Siemens SMART diffractometer fitted with a CCD-type area detector. In all cases data were collected at −100 °C to a 2θ limit of 55° using graphite-monochromatised Mo-Kα radiation. A detailed experimental description of the methods used for data collection and integration using the SMART system has been published.[19] For triclinic crystals a full sphere of data was collected to allow a good absorption correction using SADABS;[20] for all other crystal systems a hemisphere is sufficient. Table 2 contains a summary of the crystal parameters, data collection and refinement. In all cases the structures were solved by conventional heavy-atom or direct methods and refined by the full-matrix least-squares method on all F^2 data using the SHELXTL 5.03 package on a Silicon Graphics Indy computer.[21] Non-hydrogen atoms were refined with anisotropic thermal parameters; hydrogen atoms were included in calculated positions and refined with isotropic thermal parameters riding on those of the parent atom.

$[Co_2L_2(\mu\text{-}OH)_2][ClO_4]_2{\cdot}$MeCN is centrosymmetric, such that the asymmetric unit contains one half of the complex molecule, one perchlorate anion, and half of the acetonitrile molecule which is disordered over an inversion centre. $[Ni_2L_2(\mu\text{-}MeCO_2)_2][PF_6]_2{\cdot}2$dmf is likewise centrosymmetric; the structure solution and refinement presented no problems, other than the fact that the crystals diffracted rather poorly and gave broad peak profiles, which accounts for the modest level of refinement. The atoms of the dmf solvent molecule, and C(53) of the acetate, had large thermal parameters but could not be split into disordered components. The largest residual electron-density peak was located close to the methyl carbon atoms of this dmf molecule. The salt $[Cu_2L_2(\mu\text{-}OH)_2][PF_6]_2{\cdot}8$MeCN·$Et_2O$ is also centrosymmetric, but here one-quarter of the molecule is unique. There is a C_2 axis through the two metal centres and a mirror plane perpendicular to this through the two oxygen atoms. The asymmetric unit therefore contains one quarter of the complex cation, half of one hexafluorophosphate ion, two MeCN molecules and one quarter of an ether molecule (with the oxygen atom on the special position).

In $[PbL_2][ClO_4]_2{\cdot}1.5$MeCN·$0.25Et_2O$ the complex cation and the anions were well behaved. The complicated collection of

Table 1 Analytical and spectroscopic data for the new complexes

Complex	Elemental analysis[a] (%) C	H	N	FAB mass spectra, *m/z* {% intensity, suggested assignment}[b]	UV/VIS spectra[c] λ/nm (ε/dm^3 mol^{-1} cm^{-1})
$[Co_2L_2(\mu\text{-}OH)_2][ClO_4]_2$	42.9 (43.3)	3.6 (3.3)	18.7 (18.3)[d]	688 {70; $Co_2L(OH)_2(ClO_4)_2Cl$} 990 {100; $Co_2L_2(OH)_2(ClO_4)_2Cl$}	1060 (15), 512 (75), 484 (83), 328 (2400), 281 (39 000)
$[Ni_2L_2(\mu\text{-}MeCO_2)_2][PF_6]_2$	41.1 (41.4)	3.3 (3.8)	15.9 (15.4)[e]	360 {100; NiL} 379 {40; NiLF} 419 {50; $NiL(O_2CMe)$} 496 {20; $Ni_2L(O_2CMe)F$} 527 {60; unknown}[f]	990 (22), 605 (25), 286 (35 000)
$[Cu_2L_2(\mu\text{-}OH)_2][PF_6]_2$	38.7 (38.4)	3.0 (2.9)	15.3 (15.9)	730 {90; Cu_2L_2} 749 {100; Cu_2L_2F} 875 {40; $Cu_2L_2(PF_6)$} 926 {40; $Cu_2L_2(OH)_3$} 1179 {90; unknown}[f]	695 (66), 283 (35 000)
$[Zn_2L_2(\mu\text{-}OH)_2][PF_6]_2$	36.0 (36.1)	2.9 (3.3)	14.4 (14.9)[g]	385 {100; ZnLF} 518 {70; ZnL + deprotonated matrix} 619 {60; unknown}[f] 751 {50; Zn_2L_2F} 921 {40; unknown}[f]	281 (37 000)
$[PbL_2][ClO_4]_2$	40.9 (40.4)	2.8 (2.8)	16.1 (16.6)	510 {40; PbL} 609 {100; $PbL(ClO_4)$} 911 {7; $PbL_2(ClO_4)_2$}	Not measured
$[In_2LCl_4(\mu\text{-}OH)_2]$	28.1 (28.8)	1.9 (2.3)	11.5 (11.9)	No significant peaks observed	Not measured

[a] Calculated values in parentheses. [b] The *m/z* values quoted are based on the most abundant isotope. [c] Recorded in dmf. [d] Calculated analysis includes one molecule of MeCN per dinuclear complex. [e] Calculated analysis includes one molecule of dmf per dinuclear complex. [f] Isotopic pattern is consistent with a dinuclear complex. [g] Calculated analysis includes four molecules of water per dinuclear complex.

electron-density peaks corresponding to lattice solvent molecules was best modelled as a superposition of two independent MeCN molecules (0.75 site occupancy) and an ether molecule (0.25 site occupancy). No hydrogen atoms were included for these solvent molecules. The two acetonitrile molecules were refined with anisotropic thermal parameters, but the ether molecule was refined isotropically. Restraints were applied to the bond lengths and the thermal parameters of the solvent molecules to keep the refinement stable.

The complex $[In_2LCl_4(\mu\text{-}OH)_2]\cdot 3dmf$ contains in the asymmetric unit one dinuclear complex molecule (with approximate, but not crystallographic, mirror symmetry) and three independent molecules of dmf. Of these one [C(50) to O(54); see Fig. 9] is well-behaved and was refined anisotropically. The second was also refined anisotropically but with isotropic restraints, and additional restraints were applied to the positional parameters to keep the geometry sensible. Although the thermal parameters for this molecule are rather high (0.17 to 0.46 Å^2) it could not be split into disordered components. The third dmf molecule is disordered over two positions [C(70) to O(74), and C(70′) to O(74′); see Fig. 9] and was refined with 50 : 50 site occupancies, isotropic thermal parameters, and no hydrogen atoms. Restraints were applied to the geometric and thermal parameters of both disordered components, and in addition the thermal parameters of the two components were constrained to be identical, to keep the refinement stable.

CCDC reference number 186/792.

Results and Discussion

Ligand synthesis and crystal structure

The new ligand L was prepared in the conventional manner for a bis(pyrazolyl)methane, by reaction of the appropriate deprotonated pyrazole [here, 3-(2-pyridyl)pyrazole] with CH_2Br_2 under phase-transfer conditions. Two principal compounds were isolated (Scheme 1); the desired ligand L in 14% yield, and the positional isomer L′ in 10% yield in which one of the pyrazolyl rings is attached to the methylene carbon *via* N^2 rather than N^1. The poor yield is in strong contrast to that obtained for preparation of unsubstituted bpm by the same method (96%),[18] which could reflect the fact that the more conjugated nature of 3-(2-pyridyl)pyrazole will delocalise the negative charge when it is deprotonated, making it a poorer nucleophile. Also the requirement to separate L and L′ by chromatography, a problem which does not arise for bpm, resulted in some losses.

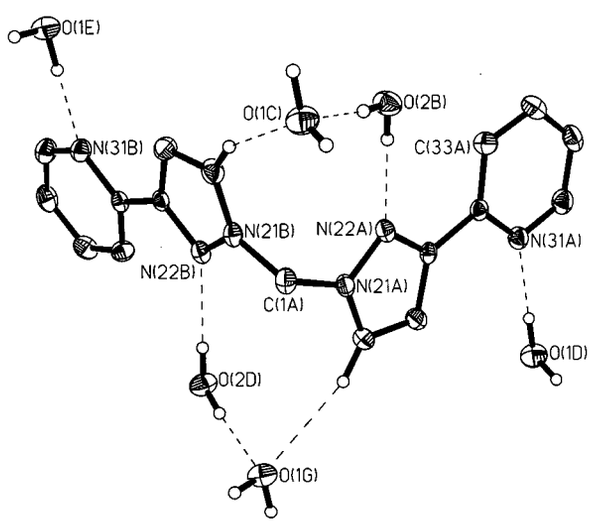

Fig. 1 Structure of $L\cdot 4H_2O$, showing the hydrogen-bonding environment around each ligand molecule. Thermal ellipsoids are at the 40% probability level

Both compounds were characterised by mass spectrometry (*m/z* = 302 in each case) and ^{1}H NMR spectroscopy. The more symmetric isomer L has two-fold symmetry and therefore seven different proton environments, whereas L′ has thirteen different proton environments. The isomer L′ clearly suffers from a greater degree of steric congestion than does L; significantly, the third possible positional isomer L″ (with both pyrazolyl groups bound to the methylene carbon *via* N^2; see Scheme 1) was not detected in the reaction mixture.

X-Ray quality crystals of L as its tetrahydrate $L\cdot 4H_2O$ were obtained, and the structure is shown in Fig. 1. The central methylene carbon atom lies on a C_2 axis, such that the two

Table 2 Summary of crystal parameters, data collection and refinement for the crystal structures

Compound	L·4H$_2$O	[Co$_2$L$_2$(μ-OH)$_2$][ClO$_4$]$_2$·MeCN	[Ni$_2$L$_2$(μ-MeCO$_2$)$_2$][PF$_6$]$_2$·2dmf	[Cu$_2$L$_2$(μ-OH)$_2$][PF$_6$]$_2$·8MeCN·Et$_2$O	[PbL$_2$][ClO$_4$]$_2$·1.5MeCN·0.25Et$_2$O	[In$_2$LCl$_4$(μ-OH)$_2$]·3dmf
Formula	C$_{17}$H$_{22}$N$_6$O$_4$	C$_{36}$H$_{33}$Cl$_2$Co$_2$N$_{13}$O$_{10}$	C$_{44}$H$_{48}$F$_{12}$N$_{14}$Ni$_2$O$_6$P$_2$	C$_{54}$H$_{64}$Cu$_2$F$_{12}$N$_{20}$O$_3$P$_2$	C$_{38}$H$_{35}$Cl$_2$N$_{13.5}$O$_{8.25}$Pb	C$_{26}$H$_{37}$Cl$_4$In$_2$N$_9$O$_5$
M	374.41	966.52	1276.32	1458.27	1090.89	927.09
System, space group	Orthorhombic, $P2_12_12$	Triclinic, $P\bar{1}$	Triclinic, $P\bar{1}$	Monoclinic, $C2/m$	Triclinic, $P\bar{1}$	Monoclinic, $P2_1/n$
a/Å	8.801(5)	7.4208(12)	10.382(2)	18.460(2)	13.530(2)	15.709(3)
b/Å	23.367(8)	11.917(3)	11.584(3)	14.512(2)	13.879(2)	11.3244(9)
c/Å	4.495(2)	12.326(4)	12.843(3)	12.314(2)	13.900(2)	21.275(2)
α/°		67.43(2)	114.51(2)		106.866(10)	
β/°		85.09(3)	96.02(2)	121.106(8)	95.538(8)	109.764(6)
γ/°		84.84(2)	108.13(2)		118.461(9)	
U/Å^3	924.3(7)	1000.9(4)	1285.9(5)	2824.4(7)	2108.8(5)	3561.9(8)
Z	2	1	1	2	2	4
D_c/g cm^{-3}	1.345	1.653	1.648	1.715	1.718	1.729
μ/mm^{-1}	0.099	1.038	0.901	0.920	4.196	1.643
F(000)	396	508	652	1496	1079	1848
Crystal size/mm	0.3 × 0.14 × 0.06	0.3 × 0.1 × 0.06	0.5 × 0.3 × 0.1	0.6 × 0.3 × 0.25	0.3 × 0.2 × 0.1	0.2 × 0.2 × 0.1
Reflections collected: total, independent, R_{int}	5462, 2113, 0.0476	10 385, 4490, 0.054	13 509, 5833, 0.038	9030, 3327, 0.033	22 120, 9542, 0.035	22 377, 8122, 0.044
2θ Limit for data/°	55	55	55	55	55	55
Data, restraints, parameters	2113, 0, 139	4490, 0, 295	5833, 0, 364	3326, 0, 231	9542, 90, 589	8120, 90, 409
Final $R1$, $wR2$ [a,b]	0.0450, 0.1024	0.0495, 0.1239	0.0765, 0.2436	0.0343, 0.0964	0.0324, 0.0675	0.0388, 0.1020
Weighting factors [b]	0.0448, 0	0.0547, 0	0.1630, 0	0.0458, 4.22	0.0292, 0	0.0525, 0
Largest peak, hole/e Å^{-3}	+0.198, −0.279	+0.679, −0.588	+1.972, −1.188	+0.549, −0.382	+0.807, −0.758	+1.062, −0.811

[a] Structure was refined on F_o^2 using all data; the value of $R1$ is given for comparison with older refinements based on F_o with a typical threshold of $F \geqslant 4\sigma(F)$. [b] $wR2 = [\Sigma w(F_o^2 - F_c^2)^2/\Sigma w(F_o^2)^2]^{\frac{1}{2}}$ where $w^{-1} = [\sigma^2(F_o^2) + (aP)^2 + bP]$ and $P = [\max(F_o^2, 0) + 2F_c^2]/3$.

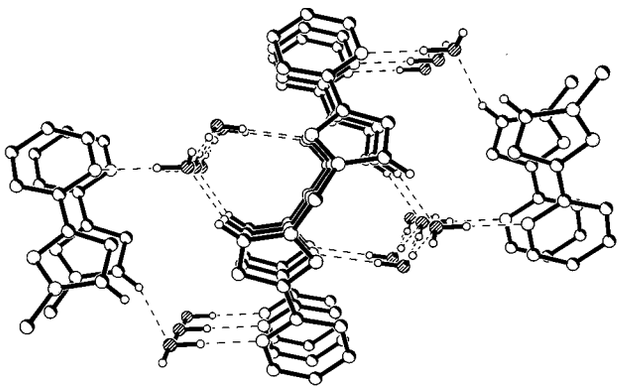

Fig. 2 Packing diagram of $L{\cdot}4H_2O$ showing the cross-linking between ligand stacks by the chains of water molecules

trans-coplanar bidentate arms are equivalent. The conformation and structural parameters of L are unremarkable. The most interesting feature of the structure is the extensive network of hydrogen bonding between the water molecules and the ligand. Fig. 1 shows the water molecules hydrogen bonded to each ligand molecule. There are three crystallographically independent interactions involving N(31) and N(22) as hydrogen-bond acceptors and H(25) as a hydrogen-bond donor; the (non-bonded) N(31)···O(1), N(22)···O(2) and C(25)···O(1) separations are 2.816(4), 2.935(4) and 3.382(4) Å respectively. There are also hydrogen bonds between water molecules, with non-bonded O···O separations of 2.754(4) and 2.710(4) Å, in the normal range for strong O–H···O interactions. The O–H···X angles (X = O, N or C) are all near-linear (170° or above). The packing diagram in Fig. 2 shows how adjacent stacks of L in the crystal are cross-linked by hydrogen bonding from the chains of water molecules.

Complexes with first-row transition-metal dications

Reaction of L with an equimolar amount of a metal(II) acetate hydrate (cobalt, nickel, copper or zinc) in methanol, followed by treatment of the resulting solutions with aqueous $NaClO_4$ or KPF_6, afforded the complexes listed in Table 1. The elemental analytical data suggested empirical formulae of the type [MLX]Y (X = hydroxide or acetate; Y = hexafluorophosphate or perchlorate as appropriate), but the FAB mass spectroscopic data clearly suggested that dinuclear complexes had formed in each case. The peaks at highest *m*/*z* value could not always be assigned with certainty, but the isotopic patterns in every case were only consistent with dinuclear complexes. For $[Co_2L_2(\mu\text{-}OH)_2][ClO_4]_2$ a molecular ion was observed corresponding to the mass of the entire complex (including perchlorate anions) plus a chloride ion, which presumably originated from fragmentation of a perchlorate. In the spectra of the Ni, Cu and Zn complexes, all of which had hexafluorophosphate as the anion, incorporation of fluoride ion could be seen in some of the fragments. The combination of elemental analyses and mass spectra suggested the dimeric formulation $[M_2L_2X_2]Y_2$ for all four complexes.

For the Ni^{II} complex, the presence of co-ordinated acetate was clear from some of the mass spectral peaks, whereas no evidence was found in the spectra of the Co^{II}, Cu^{II} and Zn^{II} complexes for the presence of acetate ions. Careful examination of the IR spectra of the three complexes showed that the Ni^{II} complex had peaks at 1636 and 1286 cm^{-1} which were not present in the other three spectra; apart from these two peaks, all three spectra were very similar with an obvious correspondence of peaks between them. The separation between these two additional peaks in the spectrum of the Ni^{II} complex (350 cm^{-1}) is consistent with the presence of monodentate acetate ions,[22] giving the overall formulation as $[Ni_2L_2(MeCO_2)_2][PF_6]_2$ in agreement with the elemental analysis. The other three complexes were tentatively formulated as $[M_2L_2(OH)_2][PF_6]_2$.

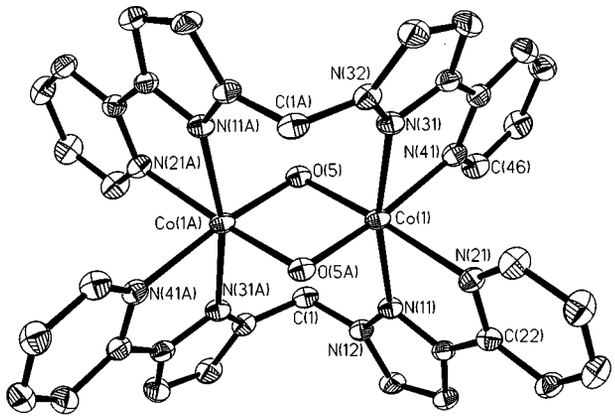

Fig. 3 Crystal structure of the complex cation of $[Co_2L_2(\mu\text{-}OH)_2][ClO_4]_2{\cdot}MeCN$. Thermal ellipsoids are at the 40% probability level

Table 3 Selected bond lengths (Å) and angles (°) for $[Co_2L_2(\mu\text{-}OH)_2][ClO_4]_2{\cdot}MeCN$ and $[Ni_2L_2(\mu\text{-}MeCO_2)_2][PF_6]_2{\cdot}2dmf$

	Co	Ni
M–O(A)*	2.035(2)	2.044(3)
M–O*	2.043(2)	2.060(3)
M–N(31)	2.172(3)	2.105(4)
M–N(11)	2.172(3)	2.094(4)
M–N(41)	2.175(3)	2.113(4)
M–N(21)	2.195(3)	2.109(4)
O(A)–M–O	88.60(10)	82.84(14)
O(A)–M–N(31)	93.42(11)	94.24(14)
O–M–N(31)	93.86(11)	92.91(14)
O(A)–M–N(11)	94.15(10)	95.08(14)
O–M–N(11)	96.35(10)	94.54(14)
N(31)–M–N(11)	167.42(11)	168.72(14)
O(A)–M–N(41)	168.83(10)	171.20(14)
O–M–N(41)	93.11(11)	94.71(14)
N(31)–M–N(41)	75.45(12)	77.4(2)
N(11)–M–N(41)	96.63(11)	93.5(2)
O(A)–M–N(21)	94.18(11)	95.5(2)
O–M–N(21)	170.88(10)	171.92(14)
N(31)–M–N(21)	94.64(11)	95.1(2)
N(11)–M–N(21)	74.81(11)	77.7(2)
N(41)–M–N(21)	85.85(12)	88.1(2)

* The generic label 'O' refers to the bridging atom: O(5) for M = Co, O(50) for M = Ni (see crystallographic numbering schemes in the appropriate figures); O(A) is its symmetry equivalent, *i.e.* the other bridging atom

The Co, Ni and Cu complexes were crystallographically characterised and all have the same basic structure, although there are significant variations between them. The structure of $[Co_2L_2(\mu\text{-}OH)_2][ClO_4]_2$ (Fig. 3, Table 3) shows that each ligand is acting as a bridge between the two metal centres, with the two ligands in a 'face-to-face' (non-helical) arrangement, and two hydroxide ions also bridging both metal centres giving a $Co_2(\mu\text{-}OH)_2$ core. Each Co^{II} centre is therefore approximately octahedrally co-ordinated by two bidentate pyridyl/pyrazolyl chelating fragments (one from each ligand L), and two (bridging) hydroxyl oxygen atoms. The Co–N bond lengths (2.172–2.195 Å) are indicative of high-spin Co^{II}, which is not surprising given the nature of the ligand donor set. Complexes $[Co(terpy)_2]X_2$ are well known to be on the high-spin/low-spin borderline,[23] and replacement of two of the aromatic N-donor ligands by hydroxide, which has a weaker ligand field, tips the balance to high-spin. The two Co–O bonds are significantly shorter (*ca.* 2.04 Å), due to the negative charges on the hydroxide ions. The Co···Co separation is 2.919(1) Å.

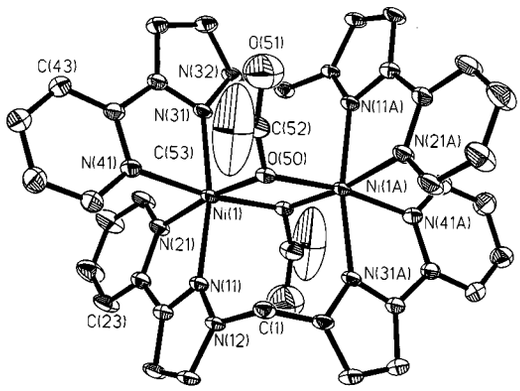

Fig. 4 Crystal structure of the complex cation of $[Ni_2L_2(\mu\text{-}MeCO_2)_2][PF_6]_2\cdot 2dmf$. Thermal ellipsoids are at the 40% probability level

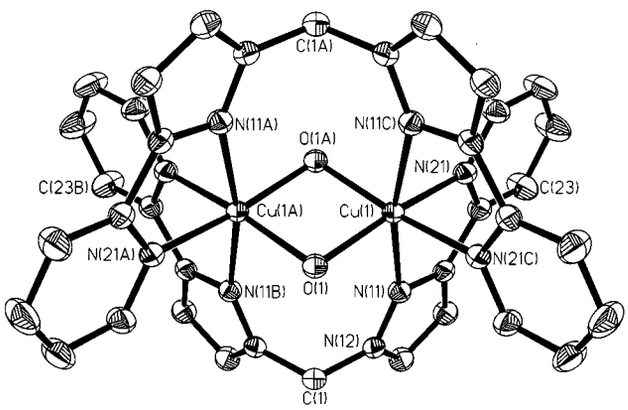

Fig. 5 Crystal structure of the complex cation of $[Cu_2L_2(\mu\text{-}OH)_2][PF_6]_2\cdot 8MeCN\cdot Et_2O$. Thermal ellipsoids are at the 40% probability level

Table 4 Selected bond lengths (Å) and angles (°) for $[Cu_2L_2(\mu\text{-}OH)_2][PF_6]_2\cdot 8MeCN\cdot Et_2O$

Cu(1)–O(1)	1.9622(13)	Cu(1)–N(11)	2.358(2)
Cu(1)–N(21)	2.079(2)		
O(1)–Cu(1)–O(1A)	84.37(8)	O(1A)–Cu(1)–N(11)	94.32(7)
O(1)–Cu(1)–N(21C)	93.76(6)	N(21)–Cu(1)–N(11)	74.84(6)
O(1)–Cu(1)–N(21)	168.35(7)	N(21)–Cu(1)–N(11C)	97.27(6)
N(21C)–Cu(1)–N(21)	90.31(9)	N(11)–Cu(1)–N(11C)	169.03(8)
O(1)–Cu(1)–N(11)	93.80(7)		

The crystal structure of the complex cation of $[Ni_2L_2(\mu\text{-}MeCO_2)_2][PF_6]_2\cdot 2dmf$ (Fig. 4, Table 3) is similar to that of the cobalt(II) complex with the exception that the hydroxide bridging ligands are replaced by monodentate acetate bridges. All metal–ligand bond lengths lie in the range 2.04–2.11 Å, with the metal–N bonds being noticeably shorter than in the cobalt(II) complex above, but the Ni–O bonds being about the same length as the Co–O bonds. The dinuclear complex cation is centrosymmetric, and the Ni · · · Ni separation is 3.077(2) Å.

The complex cation of $[Cu_2L_2(\mu\text{-}OH)_2][PF_6]_2\cdot 8MeCN\cdot Et_2O$ (Fig. 5, Table 4) again has the same basic structure seen for the other members of this series, having hydroxide rather than acetate bridging groups. The main point to note is that the co-ordination sphere of the Cu^{II} centres is distorted from octahedral geometry by the Jahn–Teller effect, with the four (equivalent) Cu–N(11) bonds, involving the pyrazolyl donors, being considerably elongated [2.358(2) Å] compared to the relatively compressed bonds on the other two axes [1.9622(13) for Cu–O and 2.079(2) Å for Cu–N(21)]. Owing to the *C*2/*m* symmetry only one quarter of the molecule is unique; there is a C_2 axis through the two metal centres and a mirror plane perpendicular to this through the two oxygen atoms. Consequently there is also an inversion centre in the middle of the $Cu_2(\mu\text{-}OH)_2$ core. The Cu · · · Cu separation is 2.908 Å, rather shorter than that in $[Ni_2L_2(\mu\text{-}MeCO_2)_2][PF_6]_2$ because of the slight equatorial compression of the Cu–O bonds which accompanies the axial elongation of the Cu–N(11) bonds, but very similar to that in $[Co_2L_2(\mu\text{-}OH)_2][ClO_4]_2$.

We obtained rather poor crystals of the zinc complex and achieved a partial structural determination. Problems occurred with refining the bridging atoms, because solvent molecules (possibly MeOH) appeared to be hydrogen bonded to the bridging hydroxide groups in an extensively disordered manner which could not be clearly modelled although the face-to-face structure of the Zn_2L_2 core was clear. For this reason the details of the structural determination are not reported, and we just note that the gross structure of $[Zn_2L_2(\mu\text{-}OH)_2][PF_6]_2$ is essentially the same as that of the other three complexes in this series.

The 'butterfly-like' arrangement of ligands L arising from their mutual face-to-face arrangement, common to all three crystal structures, is most apparent in Fig. 5. It appears to be the presence of the acetate or hydroxide bridges that result in the face-to-face arrangement; a helical arrangement of the ligands would result in a much greater degree of steric crowding in the volume of space occupied by the bridging acetates/hydroxides. With metals that have a preference for four-co-ordination (*e.g.* Cu^{I}, Ag^{I}) then a helical complex $[M_2L_2]^{2+}$ might be expected as no additional bridging ligands will be required. We attempted to prepare a Cu^{I} complex by reaction of L with $[Cu(MeCN)_4][PF_6]$ (1 : 1 ratio) in MeCN under N_2; however the resultant brown Cu^{I} complex was rather air-sensitive, becoming green in the presence of air. Further attempts to prepare helical complexes with L with monocationic metals are in progress.

Electrochemical and electronic spectroscopic properties of the transition-metal complexes

Electrochemical investigations on the complexes revealed only irreversible behaviour. For the Co^{II}, Ni^{II} and Zn^{II} complexes this occurred at extreme negative potentials, consistent with ligand-centred processes. For $[Cu_2L_2(\mu\text{-}OH)_2][PF_6]_2$ in MeCN an irreversible reduction wave at −1.65 V *vs.* the ferrocene–ferrocenium couple may be ascribed to a $Cu^{II}\rightarrow Cu^{I}$ reduction.

Electronic spectroscopic studies (Table 1) showed the expected intense ligand-centred transitions in the UV region, as well as much weaker d–d transitions for the Co^{II}, Ni^{II} and Cu^{II} complexes. For pseudo-octahedral high-spin Co^{II} complexes three d–d transitions are expected, of which the middle one [ν_2, $^4T_{1g}(F)\rightarrow{}^4A_{2g}(F)$] is often not observed as it is effectively a two-electron transition from $(t_{2g})^5(e_g)^2$ to $(t_{2g})^3(e_g)^4$ and therefore very unlikely. The transition in the near-IR region at 1060 nm is ν_1 [$^4T_{1g}(F)\rightarrow{}^4T_{2g}(F)$]; for comparison this occurs at 885 nm for $[Co(bipy)_3]^{2+}$ (bipy = 2,2′-bipyridine) and 1235 nm for $[Co(H_2O)_6]^{2+}$, and is therefore where it would be expected on the basis of relative ligand-field strengths. The transition at 484 nm is ν_3 [$^4T_{1g}(F)\rightarrow{}^4T_{1g}(P)$] and has an additional component resolved at 512 nm probably due to the considerable distortion from regular octahedral symmetry. This band is also intermediate in energy between those of $[Co(bipy)_3]^{2+}$ and $[Co(H_2O)_6]^{2+}$ (455 and 515 nm respectively).

For octahedral Ni^{II} complexes three d–d transitions are again expected, of which the highest-energy is often (as here) obscured by ligand-centred or charge-transfer transitions in the UV region. As with the Co^{II} complex, we see that the two resolved transitions [ν_1, $^3A_{2g}(F)\rightarrow{}^3T_{2g}(F)$; ν_2, $^3A_{2g}(F)\rightarrow{}^3T_{1g}(F)$] at 990 and 605 nm are intermediate in energy between the corresponding transitions for $[Ni(bipy)_3]^{2+}$ (790 and 520 nm) and $[Ni(H_2O)_6]^{2+}$ (1175 and 725 nm) in agreement with the intermediate ligand-field strength of the N_4O_2 donor set.

For Cu^{II} complexes the position and intensity of the d–d transition give a clue to the co-ordination geometry, with basically planar (or tetragonally elongated) complexes having a high-

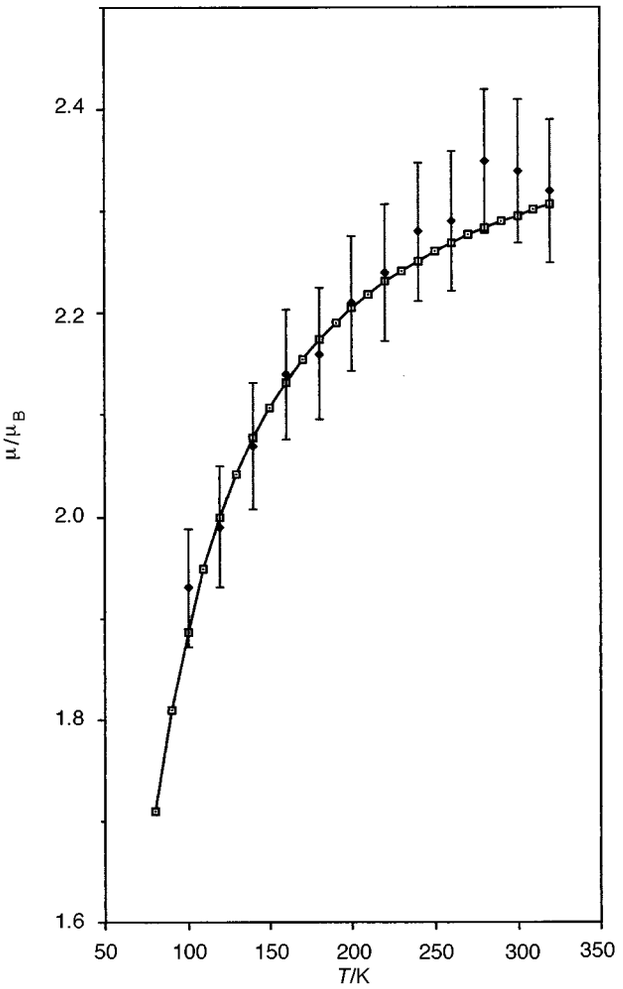

Fig. 6 Magnetic moment ($\mu_B \approx 9.274 \times 10^{-24}$ J T^{-1}) for $[Cu_2L_2(\mu\text{-}OH)_2][PF_6]_2$ as a function of temperature per dinuclear complex unit. The measured data points are black diamonds with error bars; the computed best-fit (squares with solid line through them) for $2J = -110$ cm^{-1} is also shown

energy, low-intensity band which moves to lower energy and higher intensity if tetrahedral distortions occur. The salt $[Cu_2L_2(\mu\text{-}OH)_2][PF_6]_2$ may be considered as having a basically N_2O_2 planar geometry with more remote axial N-donor ligands, and the relatively high energy and low intensity of the d–d band are entirely consistent with the solid-state structure being retained in solution.

Magnetic properties of $[Cu_2L(\mu\text{-}OH)_2][PF_6]_2$

In complexes with a $Cu^{II}_2(\mu\text{-}OH)_2$ core it is well known that magnetic exchange occurs. When there are *only* two hydroxide bridges, an accurate linear relationship exists between the magnitude of the singlet–triplet splitting $2J$ and the Cu–O–Cu angle, α [equation (1)].[24] Thus $2J$ changes sign at α = 97.5°. With

$$2J = -74.53\alpha + 7270 \text{ cm}^{-1} \quad (1)$$

larger bridging angles, the exchange interaction is antiferromagnetic; with smaller angles it is ferromagnetic. This has been rationalised by a simple molecular orbital treatment.[25] When additional bridging groups are present however, to provide additional competing pathways for superexchange, this correlation fails.[24,26]

In $[Cu_2L_2(\mu\text{-}OH)_2][PF_6]_2$ the Cu–O–Cu bridging angle is 95.63(8)°. Application of equation (1) suggests that the exchange interaction should be ferromagnetic, with $2J = +143(6)$ cm^{-1}. However a magnetic susceptibility study on this compound

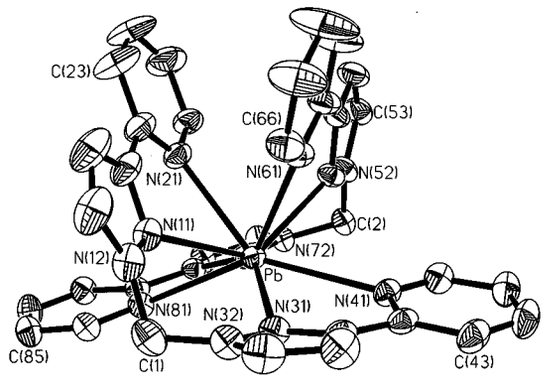

Fig. 7 Crystal structure of the complex cation of $[PbL_2][ClO_4]_2 \cdot 1.5MeCN \cdot 0.25Et_2O$. Thermal ellipsoids are at the 40% probability level

Table 5 Selected bond lengths (Å) and angles (°) for $[PbL_2][ClO_4]_2 \cdot 1.5MeCN \cdot 0.25Et_2O$

Pb–N(51)	2.626(3)	Pb–N(71)	2.778(3)
Pb–N(61)	2.639(3)	Pb–N(31)	2.830(3)
Pb–N(21)	2.647(3)	Pb–N(41)	2.871(3)
Pb–N(11)	2.687(3)	Pb–N(81)	2.910(3)
N(51)–Pb–N(61)	62.4(1)	N(21)–Pb–N(31)	126.8(1)
N(51)–Pb–N(21)	77.0(1)	N(21)–Pb–N(41)	141.2(1)
N(61)–Pb–N(21)	71.5(1)	N(21)–Pb–N(81)	73.7(1)
N(51)–Pb–N(11)	129.1(1)	N(51)–Pb–N(31)	126.9(1)
N(61)–Pb–N(11)	76.4(1)	N(51)–Pb–N(41)	74.5(1)
N(21)–Pb–N(11)	61.9(1)	N(51)–Pb–N(81)	121.7(1)
N(51)–Pb–N(71)	67.6(1)	N(61)–Pb–N(31)	80.3(1)
N(61)–Pb–N(71)	125.9(1)	N(61)–Pb–N(41)	72.2(1)
N(21)–Pb–N(71)	78.6(1)	N(61)–Pb–N(81)	142.6(1)
N(11)–Pb–N(71)	125.8(1)	N(71)–Pb–N(31)	150.8(1)
N(11)–Pb–N(31)	68.2(1)	N(71)–Pb–N(41)	113.1(1)
N(11)–Pb–N(41)	121.0(1)	N(71)–Pb–N(81)	57.9(1)
N(11)–Pb–N(81)	75.5(1)	N(31)–Pb–N(41)	58.2(1)
N(31)–Pb–N(81)	111.0(1)	N(41)–Pb–N(81)	144.6(1)

clearly indicated an antiferromagnetic interaction (Fig. 6), and fitting of the data to the Bleaney–Bowers equation gave a singlet–triplet separation of $2J = -110$ cm^{-1}. It follows that the additional bridging ligands L provide an effective pathway for antiferromagnetic exchange, despite the presence of a formally saturated sp^3 carbon atom in the pathway.

Complexes with Pb^{II} and In^{III}

We were interested to see what sort of structures the new ligand would form with p-block metal ions in contrast to d-block ions, and we used Pb^{II} and In^{III} as representative examples. The complex of L with Pb^{II} was prepared in the usual way using a 1:1 metal:ligand ratio. However the elemental analysis and FAB mass spectrum of the product were both consistent with the formulation $[PbL_2][ClO_4]_2$, *i.e.* a mononuclear complex with a 1:2 metal:ligand ratio. The crystal structure (Fig. 7, Table 5) shows that the metal has an irregular eight-co-ordinate geometry, with the Pb–N bond lengths covering the rather wide range 2.626(3) Å [Pb–N(51)] to 2.910(3) Å [Pb–N(81)], as is typical for Pb^{II} complexes.[27,28] Each ligand is not planar but, as in all the structures above, is folded about the central (pseudo-tetrahedral) methylene bridge. There is a clear gap in the co-ordination sphere which suggests the presence of a stereochemically active lone pair, which is common in Pb^{II} complexes of, amongst others, poly(pyrazolyl)borates,[27,28] and in fact this crystal structure is similar to that of $[Pb(L^1)_2]$, where L^1 is the related ligand with a BH_2 linker between the bidentate arms (Scheme 1).[28] It is noticeable that the four longest Pb–N bonds are those which are nearest to this stereochemically active lone pair. The structure contrasts strongly with the much more regular eight-co-ordinate geometries that we have observed recently

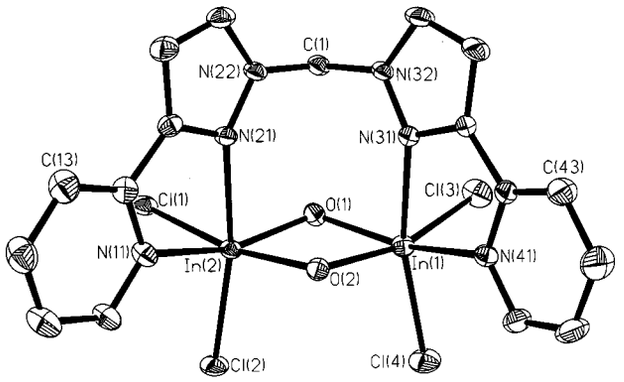

Fig. 8 Crystal structure of the complex molecule of $[In_2LCl_4(\mu\text{-}OH)_2]\cdot 3dmf$. Thermal ellipsoids are at the 40% probability level

Table 6 Selected bond lengths (Å) and angles (°) for $[In_2LCl_4(\mu\text{-}OH)_2]\cdot 3dmf$

In(1)–O(2)	2.136(3)	In(2)–O(1)	2.131(3)
In(1)–O(1)	2.168(3)	In(2)–O(2)	2.136(3)
In(1)–N(41)	2.322(4)	In(2)–N(11)	2.285(4)
In(1)–N(31)	2.366(4)	In(2)–N(21)	2.393(4)
In(1)–Cl(3)	2.4332(13)	In(2)–Cl(2)	2.4297(12)
In(1)–Cl(4)	2.4371(13)	In(2)–Cl(1)	2.4818(12)
O(2)–In(1)–O(1)	76.74(11)	O(1)–In(2)–O(2)	77.51(12)
O(2)–In(1)–N(41)	88.09(12)	O(1)–In(2)–N(11)	157.93(13)
O(1)–In(1)–N(41)	157.38(12)	O(2)–In(2)–N(11)	92.32(12)
O(2)–In(1)–N(31)	83.90(12)	O(1)–In(2)–N(21)	88.34(12)
O(1)–In(1)–N(31)	91.27(12)	O(2)–In(2)–N(21)	83.92(12)
N(41)–In(1)–N(31)	70.26(12)	N(11)–In(2)–N(21)	70.97(13)
O(2)–In(1)–Cl(3)	164.72(9)	O(1)–In(2)–Cl(2)	106.24(9)
O(1)–In(1)–Cl(3)	94.11(9)	O(2)–In(2)–Cl(2)	95.99(9)
N(41)–In(1)–Cl(3)	96.73(10)	N(11)–In(2)–Cl(2)	94.16(10)
N(31)–In(1)–Cl(3)	84.10(9)	N(21)–In(2)–Cl(2)	165.09(9)
O(2)–In(1)–Cl(4)	97.43(9)	O(1)–In(2)–Cl(1)	97.72(9)
O(1)–In(1)–Cl(4)	106.07(9)	O(2)–In(2)–Cl(1)	168.70(9)
N(41)–In(1)–Cl(4)	92.30(10)	N(11)–In(2)–Cl(1)	88.55(10)
N(31)–In(1)–Cl(4)	162.48(9)	N(21)–In(2)–Cl(1)	85.72(9)
Cl(3)–In(1)–Cl(4)	96.86(5)	Cl(2)–In(2)–Cl(1)	95.18(4)

in Pb^{II} complexes of similar ligands where the lone pair is not stereochemically active.[29]

Reaction of L with indium(III) chloride in a 1:1 ratio produced a material whose elemental analysis suggested a 2:1 metal:ligand ratio, so these proportions were used subsequently. The FAB mass spectrum of the complex gave only low molecular weight fragments, but its identity was shown to be $[In_2LCl_4(\mu\text{-}OH)_2]$ by crystallographic analysis (Fig. 8, Table 6). Each In^{III} centre has a roughly octahedral geometry with a *cis*,*cis*,*cis*-$N_2O_2Cl_2$ donor set arising from one chelating pyrazolyl/pyridine arm of L, two hydroxide groups which bridge the metal ions to give an $In_2(\mu\text{-}OH)_2$ core, and two terminal chlorides. The ligand L acts as a binucleating bridge in the same way as we saw for the transition-metal complexes, and the In···In separation is 3.3386(6) Å. The In–O bond distances in the bridge (2.13–2.17 Å), and the other bond distances, are unremarkable. Two of the lattice dmf molecules (of which one is disordered over two sites) are involved in hydrogen-bonding interactions with the bridging O–H groups (Fig. 9); the non-bonded O···O separations are 2.75 Å [O(2)···O(54)], 2.73 Å[O(1)···O(74)] and 2.79 Å [O(1)···O(74′)], which are entirely typical of O–H···O hydrogen bonds.

Most of the crystallographically characterised complexes containing $In^{III}_2(\mu\text{-}OR)_2$ fragments[30,31] are based on bridging alkoxides.[30] There are currently only three examples of such complexes with hydroxide bridges on the Cambridge Structural Database, and these are all tetranuclear clusters with adamantane-like $In_4(\mu\text{-}OH)_6$ (ref. 32) or cubane-like $In_4(\mu^3\text{-}OH)_4$ (ref. 33) cores. The complex $[In_2LCl_4(\mu\text{-}OH)_2]$ is therefore the first example of a discrete dinuclear $In^{III}_2(\mu\text{-}OH)_2$ complex.

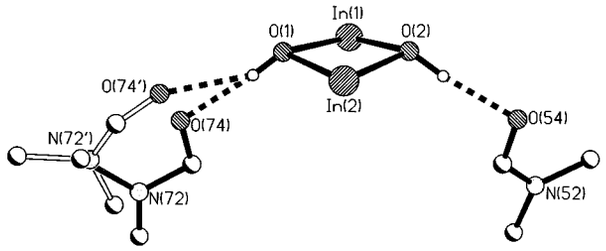

Fig. 9 Hydrogen bonding between the lattice dmf molecules and the bridging hydroxyl groups in $[In_2LCl_4(\mu\text{-}OH)_2]\cdot 3dmf$. The disordered dmf molecule [C(70)–O(74)] has 50% occupancy of two sites

Conclusion

Although L is capable of acting as a tetradentate chelate to a single metal ion if the metal is large enough, as in $[PbL_2]^{2+}$, it seems that the more usual mode of co-ordination is for L to act as a bridging ligand with each bidentate arm binding a different metal ion. The resulting separation between the two binding sites is ideal for the binding of monodentate bridging ligands between the metal ions; usually hydroxide but, in some cases, acetate. The ligand L is therefore ideal for the controlled preparation of bridged dinuclear complexes.

Acknowledgements

We thank the EPSRC for a Ph.D. studentship (to K. L. V. M.) and for a grant to purchase the diffractometer.

References

1 E. Psillakis, J. C. Jeffery, J. A. McCleverty and M. D. Ward, *J. Chem. Soc., Dalton Trans.*, 1997, 1645; D. A. Bardwell, J. C. Jeffery, P. L. Jones, J. A. McCleverty, E. Psillakis, Z. Reeves and M. D. Ward, *J. Chem. Soc., Dalton Trans.*, 1997, 2079.
2 R. W. Saalfrank, R. Harbig, J. Nachtrab, W. Bauer, K.-P. Zeller, D. Stalke and M. Teichert, *Chem. Eur. J.*, 1996, **2**, 1363; L. J. Charbonniere, G. Bernardinelli, C. Piguet, A. M. Sargeson and A. F. Williams, *J. Chem. Soc., Chem. Commun.*, 1994, 1419; C. Piguet, G. Bernardinelli, B. Bocquet, O. Schaad and A. F. Williams, *Inorg. Chem.*, 1994, **33**, 4112; A. Juris and R. Ziessel, *Inorg. Chim. Acta*, 1994, **225**, 251; C. O. Dietrich-Buchecker, J.-P. Sauvage, A. De Cian and J. Fischer, *J. Chem. Soc., Chem. Commun.*, 1994, 2231; E. C. Constable, M. J. Hannon, A. J. Edwards and P. R. Raithby, *J. Chem. Soc., Dalton Trans.*, 1994, 2669; A. F. Williams, C. Piguet and G. Bernardinelli, *Angew. Chem., Int. Ed. Engl.*, 1991, **30**, 1490; M. T. Youninou, R. Ziessel and J.-M. Lehn, *Inorg. Chem.*, 1991, **30**, 2144; A. Bilyk and M. M. Harding, *J. Chem. Soc., Chem. Commun.*, 1995, 1697.
3 E. Psillakis, J. C. Jeffery, J. A. McCleverty and M. D. Ward, *Chem. Commun.*, 1997, 479.
4 A. Bilyk, M. M. Harding, P. Turner and P. W. Hambley, *J. Chem. Soc., Dalton Trans.*, 1994, 2783; C. O. Dietrich-Buchecker, J.-P. Sauvage, J.-P. Kintzinger, P. Maltese, C. Pascard and J. Guilhem, *New J. Chem.*, 1992, **16**, 931; C. O. Dietrich-Buchecker, J. F. Nierengarten, J.-P. Sauvage, N. Armaroli, V. Balzani and L. De Cola, *J. Am. Chem. Soc.*, 1993, **115**, 112 37.
5 P. L. Jones, K. J. Byrom, J. C. Jeffery, J. A. McCleverty and M. D. Ward, *Chem. Commun.*, 1997, 1361.
6 B. Hasenknopf, J.-M. Lehn, B. O. Kneisel, G. Baum and D. Fenske, *Angew. Chem., Int. Ed. Engl.*, 1996, **35**, 1838.
7 D. Philp and J. F. Stoddart, *Angew. Chem., Int. Ed. Engl.*, 1996, **35**, 1155; J.-M. Lehn, *Supramolecular Chemistry*, VCH, Weinheim, 1995.
8 M. D. Ward, *Chem. Soc. Rev.*, 1995, **24**, 121.
9 V. A. Ung, A. M. W. Cargill Thompson, D. A. Bardwell, D. Gatteschi, J. C. Jeffery, J. A. McCleverty, F. Totti and M. D. Ward, *Inorg. Chem.*, 1997, **36**, 3447.
10 W. Kaim and B. Schwederski, *Bioinorganic Chemistry: Inorganic Elements in the Chemistry of Life*, Wiley, Chichester, 1995.
11 S. Trofimenko, *J. Am. Chem. Soc.*, 1970, **92**, 5118.

12 C. Pettinari, A. Lorenzotti, G. Sclavi, A. Cingolani, E. Rivarola, M. Colapietro and A. Cassetta, *J. Organomet. Chem.*, 1995, **496**, 69; C. Pettinari, G. G. Lobbia, A. Lorenzotti and A. Cingolani, *Polyhedron*, 1995, **14**, 793; A. E. Corrochano, F. A. Jalon, A. Otero, M. M. Kubicki and P. Richard, *Organometallics*, 1997, **16**, 145; F. A. Jalón, B. R. Manzano, A. Otero and M. C. Rodríguez-Pérez, *J. Organomet. Chem.*, 1995, **494**, 179; M. Fajardo, A. de la Hoz, E. Diéz-Barra, F. A. Jalón, A. Otero, A. Rodriguez, J. Tejeda, D. Belletti, M. Lanfranchi and M. A. Pellinghelli, *J. Chem. Soc.*, *Dalton Trans.*, 1993, 1935.
13 T. Astley, M. A. Hitchman, B. W. Skelton and A. H. White, *Aust. J. Chem.*, 1997, **50**, 145; H. Vahrenkamp and R. Alsfasser, *Inorg. Chim. Acta*, 1993, **209**, 19.
14 T. C. Higgs and C. J. Carrano, *Inorg. Chem.*, 1997, **36**, 291; 298.
15 A. M. W. Cargill Thompson, D. A. Bardwell, J. C. Jeffery, L. H. Rees and M. D. Ward, *J. Chem. Soc.*, *Dalton Trans.*, 1997, 721.
16 A. J. Amoroso, A. M. W. Cargill Thompson, J. C. Jeffery, P. L. Jones, J. A. McCleverty and M. D. Ward, *J. Chem. Soc.*, *Chem. Commun.*, 1994, 2751; H. Brunner and T. Scheck, *Chem. Ber.*, 1992, **125**, 701.
17 M. A. Laffey and P. Thornton, *J. Chem. Soc.*, *Dalton Trans.*, 1982, 313.
18 V. S. Joshi, A. Sarkar and P. R. Rajamohanan, *J. Organomet. Chem.*, 1991, **409**, 341.
19 P. L. Jones, A. J. Amoroso, J. C. Jeffery, J. A. McCleverty, E. Psillakis, L. H. Rees and M. D. Ward, *Inorg. Chem.*, 1997, **36**, 10.
20 G. M. Sheldrick, SADABS, Empirical Absorption Corrections Program, University of Göttingen, 1996.
21 SHELXTL 5.03 program system, Siemens Analytical X-Ray Instruments, Madison, WI, 1995.
22 K. Nakamoto, *Infrared and Raman Spectra of Inorganic and Coordination Compounds*, Wiley, New York, 4th edn., 1986, p. 232.
23 B. Whittle, E. L. Horwood, L. H. Rees, S. R. Batten, J. C. Jeffery and M. D. Ward, *Polyhedron*, in the press.
24 V. H. Crawford, H. W. Richardson, J. R. Wasson, D. J. Hodgson and W. E. Hatfield, *Inorg. Chem.*, 1976, **15**, 2107.
25 D. J. Hodgson, *Prog. Inorg. Chem.*, 1975, **19**, 173.
26 L. K. Thompson, S. K. Mandal, S. S. Tandon, J. N. Bridson and M. K. Park, *Inorg. Chem.*, 1996, **35**, 3117.
27 P. L. Jones, K. L. V. Mann, J. C. Jeffery, J. A. McCleverty and M. D. Ward, *Polyhedron*, 1997, **16**, 2435.
28 D. A. Bardwell, J. C. Jeffery, J. A. McCleverty and M. D. Ward, *Inorg. Chim. Acta*, 1997, in the press.
29 E. Psillakis, J. C. Jeffery, J. A. McCleverty and M. D. Ward, *Chem. Commun.*, 1997, 1965.
30 D. J. Rose, Y. D. Chang, Q. Chen, P. B. Kettler and J. Zubieta, *Inorg. Chem.*, 1995, **34**, 3973; A. J. Canty, L. A. Titcombe, B. W. Skelton and A. H. White, *J. Chem. Soc.*, *Dalton Trans.*, 1988, 35; K. Hegetschweiler, M. Ghisletta, T. F. Fässler and R. Nesper, *Angew. Chem.*, *Int. Ed. Engl.*, 1993, **32**, 1426; D. C. Bradley, H. Chudzynska, D. M. Frigo, M. E. Hammond, M. B. Hursthouse and M. A. Mazid, *Polyhedron*, 1990, **9**, 719; D. C. Bradley, D. M. Frigo, M. B. Hursthouse and B. Hussain, *Organometallics*, 1988, **7**, 1112; U. Dembowski, T. Pape, R. Herbst-Irmer, E. Pohl, H. W. Roesky and G. M. Sheldrick, *Acta Crystallogr.*, *Sect. C*, 1993, **49**, 1309.
31 N. W. Alcock, I. A. Degnan, S. M. Roe and M. G. H. Wallbridge, *J. Organomet. Chem.*, 1991, **414**, 285; T. A. Annan, J. Gu, Z. Tian and D. G. Tuck, *J. Chem. Soc.*, *Dalton Trans.*, 1992, 3061; T. A. Annan, M. A. Brown, A. El-Hadad, B. R. McGarvey, A. Ozarowski and D. G. Tuck, *Inorg. Chim. Acta*, 1994, **225**, 207; W. M. Cleaver and A. R. Barron, *J. Am. Chem. Soc.*, 1989, **111**, 8966; A. G. Groves, W. T. Robinson and C. J. Wilkins, *Inorg. Chim. Acta*, 1986, **114**, L29.
32 S. S. Al-Juaid, N. H. Buttruss, C. Eaborn, P. B. Hitchcock, A. T. L. Roberts, J. D. Smith and A. C. Sullivan, *J. Chem. Soc.*, *Chem. Commun.*, 1986, 908; K. Wieghardt, M. Kleine-Boymann, B. Nuber and J. Weiss, *Inorg. Chem.*, 1986, **25**, 1654.
33 A. M. Arif and A. R. Barron, *Polyhedron*, 1988, **7**, 2091.

Received 19*th September* 1997; *Paper* 7/06806I